

Dynamical patterns of epidemic outbreaks in complex heterogeneous networks

Marc Barthélemy^{a,*}, Alain Barrat^b, Romualdo Pastor-Satorras^c, Alessandro Vespignani^{b,d}

^aCEA-Centre d'Etudes de Bruyères-le-Châtel, Département de Physique Théorique et Appliquée BP12, 91680 Bruyères-Le-Châtel, France

^bLaboratoire de Physique Théorique (UMR du CNRS 8627), Bâtiment 210 Université de Paris-Sud, 91405 Orsay, France

^cDepartament de Física i Enginyeria Nuclear, Universitat Politècnica de Catalunya Campus Nord, 08034 Barcelona, Spain

^dSchool of Informatics and Biocomplexity Center, Indiana University, Bloomington, IN 47408, USA

Received 13 October 2004; accepted 18 January 2005

Available online 10 March 2005

Abstract

We present a thorough inspection of the dynamical behavior of epidemic phenomena in populations with complex and heterogeneous connectivity patterns. We show that the growth of the epidemic prevalence is virtually instantaneous in all networks characterized by diverging degree fluctuations, independently of the structure of the connectivity correlation functions characterizing the population network. By means of analytical and numerical results, we show that the outbreak time evolution follows a precise hierarchical dynamics. Once reached the most highly connected hubs, the infection pervades the network in a progressive cascade across smaller degree classes. Finally, we show the influence of the initial conditions and the relevance of statistical results in single case studies concerning heterogeneous networks. The emerging theoretical framework appears of general interest in view of the recently observed abundance of natural networks with complex topological features and might provide useful insights for the development of adaptive strategies aimed at epidemic containment.

© 2005 Elsevier Ltd. All rights reserved.

Keywords: Complex networks; Disease spreading; Epidemic modeling

1. Introduction

Accurate mathematical models of epidemic spreading are the basic conceptual tools in understanding the impact of diseases and the development of effective strategies for their control and containment (Bailey, 1975; Anderson and May, 1992; Diekmann and Heesterbeek, 2000; Dailey and Gani, 2001). In order to increase the relevance and utility of these strategies, it is crucial that models contain the key features that appropriately characterize the system of interest. The age and social structure of the population, the contact network among individuals, and the meta-

population characteristics such as the geographical patch structure, are all factors that might acquire a particular relevance in a reliable epidemic model (for a recent review on the subject see (Ferguson et al., 2003)). Among these features, the connectivity pattern of the network of contacts among individuals along which the disease can be transmitted has been acknowledged since a long time as a relevant factor in determining the properties of epidemic spreading phenomena (see Yorke et al., 1978; Hethcote and Yorke, 1984; May and Anderson, 1988; Anderson and May, 1992; Eubank et al., 2004 and references therein). In these studies, it was observed that the heterogeneity of the population network in which the disease spreads may have noticeable effects in the evolution of the epidemic as well as in the effect of immunization strategies.

*Corresponding author. Tel.: +33 1 69 265959;
fax: +33 1 69 267106.

E-mail address: marc.barthelemy@th.u-psud.fr (M. Barthélemy).

The study of the impact of network structure in the epidemic modeling has been recently revamped by the large number of results on large networked systems pointing out the ubiquitous presence of heterogeneities and complex topological features on a wide range of scales (Albert and Barabási, 2002; Dorogovtsev and Mendes, 2003; Pastor-Satorras and Vespignani, 2004). A striking example of this new framework is provided by scale-free networks, which are characterized by virtually infinite fluctuations in the number of connections k (the degree) that any given vertex in the network may have. This feature finds its signature in a heavy-tailed degree distribution (defined as the probability that any vertex is connected to k other vertices), often approximated by a power-law behavior of the form $P(k) \sim k^{-\gamma}$, with $2 < \gamma \leq 3$. This implies an unexpected statistical abundance of vertices with very large degrees; i.e. the so called “hubs” or “superspreaders” (Yorke et al., 1978). In heavy-tailed networks the abundance of those vertices reaches a level that guarantees the proliferation of a large number of infected individuals whatever the rate of infection characterizing the epidemic, eventually leading to the absence of any epidemic threshold below which the infection cannot initiate a major outbreak (Pastor-Satorras and Vespignani, 2001a,b; May and Lloyd, 2001; Moreno et al., 2002; Newman, 2001). This peculiar theoretical scenario, however, turns out to be of practical importance since both the sexual contact pattern (Colgate et al., 1989; Liljeros et al., 2001; Schneeberger et al., 2004) and several technological networks (Pastor-Satorras and Vespignani, 2001a; Lloyd and May, 2001; Pastor-Satorras and Vespignani, 2004) appear to have a skewed and heavy-tailed degree distribution. This implies that both sexually transmitted diseases and computer viruses may fit in this scenario, raising new questions and scrutiny on several epidemic models and strategies aimed at optimizing the deployment of immunization resources (Dezsö and Barabási, 2002; Cohen and Havlin, 2003).

In this paper, we provide a thorough presentation of results concerning the analysis of the time evolution of epidemic outbreaks in complex networks with highly heterogeneous connectivity patterns. We consider the time behavior of epidemic outbreaks in the general class of models without and with internal recovery and find that the growth of infected individuals is governed by a time-scale τ proportional to the ratio between the first and second moment of the network's degree distribution (Barthélemy et al., 2004), $\tau \sim \langle k \rangle / \langle k^2 \rangle$. This implies that the larger the degree fluctuations (governed by $\langle k^2 \rangle$), the faster the epidemic propagation will be. In particular, a virtually instantaneous rise of the prevalence is obtained in scale-free networks where $\langle k^2 \rangle \rightarrow \infty$ for infinite network sizes. This result is shown to be valid also in networks with non-trivial connectivity correlation functions as often encountered in real systems analysis. Furthermore, we study the detailed propagation in time

of the infection through the different degree classes in the population. We find a striking hierarchical dynamics in which the infection propagates via a cascade that progresses from higher to lower degree classes. This infection hierarchy might be used to develop dynamical ad hoc strategies for network protection. Finally, we study the influence of initial conditions on the epidemic development and the relevance of statistical results in the case of single case studies. All the analytical discussion is supplemented with careful numerical simulations at the discrete individual level.

2. Basic theory of epidemic dynamics

2.1. Reproductive number and time evolution

At first instance epidemiological studies deal with the properties of epidemics in the equilibrium or long-time steady state such as a non-zero prevalence state associated to the presence of an endemic phase, the presence or absence of a global outbreak, or the non-seasonal cycles that are observed in many infections (Anderson and May, 1992). As well, the dynamical evolution of epidemics outbreaks and the effects of the introduction of a seed of infection into a large population of susceptible individuals are of great concern. A basic parameter in epidemiology is the basic reproductive number R_0 , which counts the number of secondary infected cases generated by one primary infected individual. Under the assumption of the homogeneous mixing of the population if an infected individual is in contact with $\langle k \rangle$ other individual, the basic reproductive number is defined as

$$R_0 = \frac{\lambda \langle k \rangle}{\mu}, \quad (1)$$

where λ is the spreading rate, defined as the probability rate that a susceptible individual in contact with an infected individual will contract the disease, and μ is the recovery rate of infected individuals, either to the susceptible or the recovered states. It is easy to understand that any epidemic will spread across a non-zero fraction of the population only for $R_0 > 1$. In this case the epidemic is able to generate a number of infected individuals larger than those which are recovered, leading to an increase of the infected individuals $i(t)$ at time t following the exponential form

$$i(t) \simeq i_0 e^{t/\tau_d}. \quad (2)$$

Here i_0 is the initial density of infected individuals and τ_d is the typical outbreak time, that in general reads as (Anderson and May, 1992)

$$\tau_d^{-1} = \mu(R_0 - 1). \quad (3)$$

The previous considerations lead to the definition of a crucial epidemiological concept, namely the epidemic threshold. Indeed, if the spreading rate is not large enough to allow a reproductive number larger than one ($\lambda > \mu/\langle k \rangle$), the epidemic outbreak will not affect a finite portion of the population and dies out in a finite time. In epidemiological studies for which the two important assumptions of “homogeneous mixing” and constant infectiousness (constant λ) are made, the spreading pattern of the epidemics is therefore controlled by the generation time-scale $1/\lambda$ and R_0 and there are roughly three different stages in an epidemics (Ferguson et al., 2003). More precisely, when infectious individuals are introduced in a network, one observes a first noisy phase followed in general by an exponential outbreak of the epidemics. Depending on the long-term behavior of individuals against the disease we will observe at large times a different behavior described by the specific epidemic model used (see Fig. 1).

The above considerations and parameters are at the core of several epidemic models based on the compartmentalization of the population. In other words, each individual of the population can only exist in a certain number of discrete states such as susceptible, infected or permanently recovered. The latter state is equivalent to the removal of the individual from the population since it is supposed that it cannot get the infection anymore. The total population N is assumed to be constant and if $S(t)$, $I(t)$ and $R(t)$ are the number of susceptible, infected and removed individuals at time t , respectively, then $N = S(t) + I(t) + R(t)$. The simplest epidemiological model one can consider is the susceptible-infected-susceptible (SIS) model. The SIS model is mainly used as a paradigmatic model for the study of infectious diseases leading to an endemic state with a stationary and constant value for the prevalence of

infected individuals, i.e. the degree to which the infection is widespread in the population. In the SIS model, individuals can only exist in two discrete states, namely, susceptible and infected. The disease transmission is described in an effective way. The probability that a susceptible vertex acquires the infection from any given neighbor in an infinitesimal time interval dt is λdt , where λ defines the virus spreading rate. At the same time, infected vertices are cured and become again susceptible with probability μdt . Individuals thus run stochastically through the cycle susceptible \rightarrow infected \rightarrow susceptible, hence the name of the model. The SIS model does not take into account the possibility of individuals removal due to death or acquired immunization, which would lead to the so-called susceptible-infected-removed (SIR) model (Anderson and May, 1992; Murray, 1993). The SIR model, in fact, assumes that infected individuals disappear permanently from the network with rate μ . In models such as the SIS, the number of infected individuals increases up to a stationary constant value which is non-zero if $R_0 > 1$. On the contrary, in models such as the SIR, the number of infected individuals tends toward zero since all infected will sooner or later become removed from the population. Also in this case, however, a finite fraction of the population is affected by the epidemic outbreak only if $R_0 > 1$. It should be noted that it is also possible to induct a steady state in the SIR model, by introducing new susceptible individuals at a constant rate. This new parameter constitutes a new time-scale that gives rise to oscillations in the endemic phase (May and Anderson, 1984).

2.2. Complex heterogeneous networks

The general picture presented in the previous section is obtained in the framework of the homogeneous mixing hypothesis. This hypothesis assumes that the network of contacts among individuals has very small degree fluctuations. In other words, the degree k fluctuates very little and we can assume $k \simeq \langle k \rangle$, where the brackets $\langle \cdot \rangle$ denote the average over the degree distribution.

However, networks can be very heterogeneous. Social heterogeneity and the existence of “super-spreaders” have been known for long time in the epidemics literature (Hethcote and Yorke, 1984). The signature of this large heterogeneity can be measured in the degree distribution $P(k)$ which in this case decays very slowly. Indeed, in a homogeneous network such as a random graph (Erdős and Rényi, 1959), $P(k)$ decays faster than exponentially, while for scale-free networks (Albert and Barabási, 2002) it decays as a power law for large k

$$P(k) \sim k^{-\gamma}. \quad (4)$$

Examples of such networks relevant to epidemics studies include the Internet (Pastor-Satorras and Vespignani,

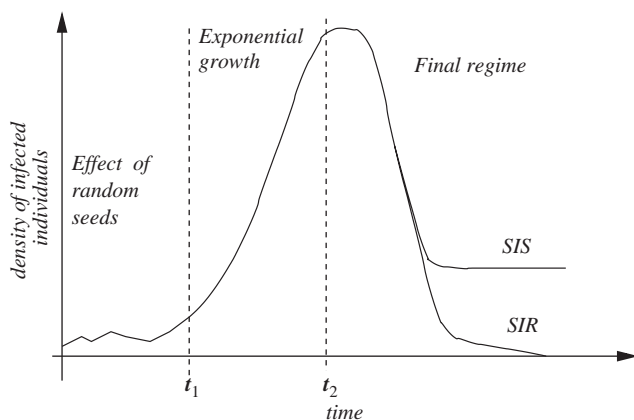


Fig. 1. Typical profile of density of infected versus time on a given realization of the network. In the first regime $t < t_1$, the outbreak did not start and there are fluctuations. In the second regime, $t_1 < t < t_2$ there is an exponential growth characterized by R_0 . In the final regime ($t > t_2$), the density of infected either converges to a constant for the SIS model or to zero for the SIR model.

2004), the network of airline connections (Guimerà et al., 2003; Barrat et al., 2004), or the web of sexual contacts (Colgate et al., 1989; Liljeros et al., 2001; Schneeberger et al., 2004). In these networks, the average degree (k) is no longer the relevant variable and one expects the fluctuations, described by $\langle k^2 \rangle$, to play an important role.

The question of the effect of the heterogeneity on epidemic behavior has been addressed at various levels (Hethcote and Yorke, 1984) and analysed in details in the last years for scale-free networks (Pastor-Satorras and Vespignani, 2001a,b). These studies were concerned with the stationary limit and the existence of an endemic phase. A key result is the expression of the basic reproductive number which in this case takes the form

$$R_0 \propto \frac{\langle k^2 \rangle}{\langle k \rangle}. \quad (5)$$

The important fact here is that R_0 is proportional to the second moment of the degree, which diverges for increasing network sizes. This has some important epidemiological consequences. Indeed, whatever the spreading rate λ the basic reproductive rate is always larger than one, thus leading to the lack of any epidemic threshold. In other words, in heterogeneous networks, whatever the infection rate, the epidemics has a finite probability to generate a major outbreak.

These results, while extremely important, consider only one face of networks complexity. In general, however, real networks have other complex features such as strong degree correlation among connected vertices. This feature is mathematically characterized through the conditional probability $P(k'|k)$ that a vertex of degree k is connected to a vertex of degree k' . Networks which are completely defined by the degree distribution $P(k)$ and the conditional probability $P(k'|k)$ are called *Markovian networks* (Boguñá and Pastor-Satorras, 2002) and must fulfill the following degree detailed balance condition

$$kP(k'|k)P(k) = k'P(k|k')P(k'). \quad (6)$$

This expression is a mathematical statement of the obvious observation that, in any real network, all edges must point from one vertex to another.

The full knowledge of the function $P(k'|k)$, which measures the correlations in the network, would often be difficult to interpret. Therefore, the *average nearest neighbor degree* k_{nn} , and the behavior of this quantity as a function of the degree, $k_{nn}(k) = \sum_{k'} k' P(k'|k)$, have been proposed to measure these correlations (Pastor-Satorras and Vespignani, 2004). In the absence of degree correlations, $P(k'|k)$ does not depend on k and neither does the average nearest neighbors' degree; i.e. $k_{nn}(k) = \text{const.}$ (Pastor-Satorras and Vespignani, 2004). In the presence of correlations, the behavior of $k_{nn}(k)$ identifies two general classes of networks. If $k_{nn}(k)$ is an increasing

function of k , vertices with high degree have a larger probability to be connected with large degree vertices. This property is referred in physics and social sciences as *assortative mixing* (Newman, 2002a,b). On the contrary, a decreasing behavior of $k_{nn}(k)$ defines *disassortative mixing*, in the sense that high-degree vertices have a majority of neighbors with low degree, while the opposite holds for low-degree vertices. These possibilities are summarized in Fig. 2. Among real networks, many social networks display assortative mixing, while technological networks show typically disassortative properties. In summary, the average nearest neighbor degree carry an information about two-point correlations which is easy to interpret and avoids the fine details of the full distribution $P(k'|k)$.

The propagation of epidemics on a network may a priori be modified by the presence of correlations. The quantity k_{nn} seems in this context very relevant, since it measures the number of individuals that may be reached by the infection in few steps. In general, however, it has been shown in (Boguñá et al., 2003a,b) that, in any scale-free network with diverging second moment $\langle k^2 \rangle$, the epidemic threshold of the model vanishes, regardless of the presence of correlations. In finite networks, the role of correlations appears through the fact that the epidemic threshold is bounded from above by a quantity which depends on k_{nn} (Boguñá et al., 2003a,b).

While these results contribute to a general understanding of epidemic spreading in complex networks, they do not provide a large amount of information about the time patterns of the dynamical process and how effectively the spreading occurs. Uncovering these patterns and their relation to the heterogeneity of the networks is crucial for assessing control strategies. In the following sections we will approach this problem within a general formalism, valid for most kind of epidemic processes in heterogeneous networks.

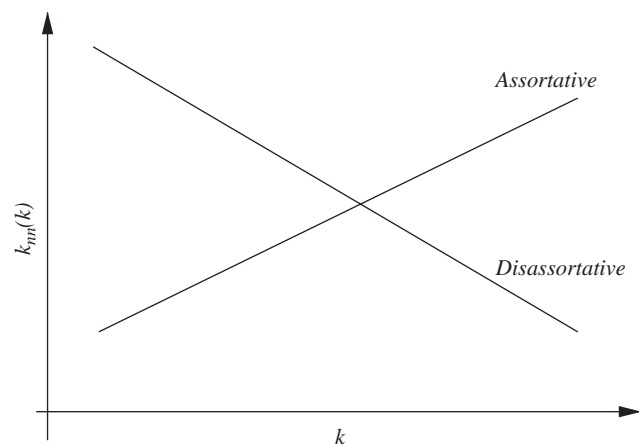


Fig. 2. Typical behavior of the average nearest neighbor degree $k_{nn}(k)$ for assortative mixing and disassortative mixing.

3. The early stages of the epidemic outbreak

In order to understand how the topology of the network of contacts affects the dynamical process of epidemics spreading, we will perform a study on different kinds of networks. Most complex networks can be classified according to the decay of their degree distribution (Amaral et al., 2000). We will first consider the case where the degree distribution decays faster than any power-law, typically as an exponential (or faster), such as for the random (Poisson) graph (Erdős and Rényi, 1959). For this sort of networks, the degree fluctuations are very small and we can approximate the degree of every vertex as a constant, $k \approx \langle k \rangle$. This approximation, used in most previous studies (Anderson and May, 1992; Murray, 1993), corresponds to the homogeneous mixing case in which all individuals have the same environment, and the same number of acquaintances that can be infected. We will then consider the case of heterogeneous networks, exemplified in the case of the scale-free networks, and show how the large heterogeneity induces changes in the epidemic process.

Both the SIS and SIR models introduce a time-scale $\tau_r = 1/\mu$ governing the self-recovery of individuals. Since we are especially interested in the onset dynamics of outbreaks two scenarios are in order. If τ_r is smaller than the spreading time-scale, then the process is dominated by the natural recovery of infected to susceptible or removed individuals. This situation is however less interesting since it corresponds to a dynamic process governed by the decay into a healthy state and the interaction with neighbors plays a minor role. Epidemiological concern is therefore in the regime $\tau_r \gg 1/\lambda$; i.e. a spreading time-scale much smaller than the recovery time-scale. In this case, as a first approximation, we can neglect the individual recovery that will occur at a much later stage and focus on the early dynamics of the epidemic outbreak. This case corresponds to the simplified susceptible-infected (SI) model, for which infected nodes remain always infective and spread the infection to susceptible neighbors with rate λ ; the seed of infectives placed at time $t = 0$ will thus infect the rest of the network, the dynamical process being controlled by the topology of the network. The SI model thus appears as the simplest framework for assessing the effect of network's topology on the spreading dynamics. This argument is the reason why we will present our calculations for the simple SI model. For the sake of completeness, however, we will readily show in the next sections that the results obtained for the SI model can be considered as fairly general and can be easily extended to SIS and SIR models for heterogeneous networks.

3.1. Homogeneous networks

A first analytical description of the SI model can be undertaken within the homogeneous mixing hypothesis (Anderson and May, 1992; Murray, 1993), consisting in a mean-field description of the system in which all vertices are considered as being equivalent. In this case the system is completely defined by the number of infected individual $I(t)$, and the reaction rate equation for the density of infected individuals $i(t) = I(t)/N$ (where N is the total size of the population) reads as

$$\frac{di(t)}{dt} = \lambda \langle k \rangle i(t) [1 - i(t)]. \quad (7)$$

The above equation states that the growth rate of infected individuals is proportional to the spreading rate λ , the density of susceptible vertices that may become infected, $s(t) = 1 - i(t)$, and the number of infected individuals in contact with any susceptible vertex. The homogeneous mixing hypothesis considers that this last term is simply the product of the number of neighbors $\langle k \rangle$ and the average density $i(t)$. Obviously, this approximation neglects correlations among individuals and considers that all vertices have the same number of neighbors $\langle k \rangle$, i.e. it assumes a perfectly homogeneous network. The solution of Eq. (7) reads

$$i(t) = \frac{i_0 \exp(t/\tau_H)}{1 + i_0 [\exp(t/\tau_H) - 1]}, \quad (8)$$

where i_0 is the initial density of infected individuals and $\tau_H = (\lambda \langle k \rangle)^{-1}$ is the time-scale of the infection growth. At small times, when the density of infected vertices is very small, the leading behavior is given by $i(t) \simeq i_0 e^{t/\tau_H}$, i.e. by an exponential growth. The value of τ_H corresponds to the intuitive fact that small spreading rates decrease the growth velocity, while a larger number of neighbors ensures a faster invasion of the network.

3.2. Heterogeneous networks

The above calculations are valid for networks in which the degree fluctuations are very small, i.e. $k \approx \langle k \rangle$ for all vertices in the network. We face however a different situation in networks with a heterogeneous connectivity pattern. In this case the degree k of vertices is highly fluctuating and the average degree is not anymore a meaningful characterization of the network properties. In order to take this into account, it is possible to write down the reaction rate equations for the densities of infected vertices of degree k , $i_k(t) = I_k(t)/N_k$, where N_k (resp. $I_k(t)$) is the number of vertices (resp. infected vertices) within each degree class k (Pastor-Satorras and Vespignani, 2001a). In the case of the SI model the evolution

equations read (Boguñá et al., 2003a,b)

$$\frac{di_k(t)}{dt} = \lambda[1 - i_k(t)]k\Theta_k(t), \tag{9}$$

where the creation term is proportional to the spreading rate λ , the degree k , the probability $1-i_k$ that a vertex with degree k is not infected, and the density Θ_k of infected neighbors of vertices of degree k . The latter term is thus the average probability that any given neighbor of a vertex of degree k is infected.

The simplest situation one can encounter corresponds to a complete lack of correlations (We will address the case of correlated networks in Section 3.4). A network is said to have no degree correlations when the probability that an edge departing from a vertex of degree k arrives at a vertex of degree k' is independent of the degree of the initial vertex k . In this case, the probability that each edge of a susceptible is pointing to an infected vertex of degree k' is proportional to the fraction of edges emanated from these vertices. Moreover, each infected vertex can either be one of the initial seeds or be infected at $t > 0$. In the latter case, at least one of the edges of the infected vertex is pointing to another infected vertex, from which the infection has been transmitted. The term Θ is therefore the sum of two terms

$$\Theta_k(t) = \Theta(t) = \frac{\sum_{k'} k' P(k') i_{k'}(0)}{\langle k \rangle} + \frac{\sum_{k'} (k' - 1) P(k') (i_{k'}(t) - i_{k'}(0))}{\langle k \rangle}, \tag{10}$$

where $\langle k \rangle = \sum_{k'} k' P(k')$ is the proper normalization factor dictated by the total number of edges.

A reaction rate equation for $\Theta(t)$ can be obtained from Eqs. (9) and (10). In the initial epidemic stages, neglecting terms of order $\mathcal{O}(i^2)$, the following set of equations is obtained

$$\frac{di_k(t)}{dt} = \lambda k \Theta(t), \tag{11}$$

$$\frac{d\Theta(t)}{dt} = \lambda \left(\frac{\langle k^2 \rangle}{\langle k \rangle} - 1 \right) \Theta(t). \tag{12}$$

These equations can be solved, yielding for the prevalence of nodes of degree k , in the case of an uniform initial condition $i_k(t=0) = i_0$,

$$i_k(t) = i_0 \left[1 + \frac{k \langle k \rangle}{\langle k^2 \rangle - \langle k \rangle} (e^{t/\tau} - 1) \right] \tag{13}$$

and for the total average prevalence $i(t) = \sum_k P(k) i_k(t)$

$$i(t) = i_0 \left[1 + \frac{\langle k \rangle^2}{\langle k^2 \rangle - \langle k \rangle} (e^{t/\tau} - 1) \right], \tag{14}$$

where

$$\tau = \frac{\langle k \rangle}{\lambda(\langle k^2 \rangle - \langle k \rangle)}. \tag{15}$$

The result Eq. (15) for uncorrelated networks readily implies that the growth time-scale of an epidemic outbreak is related to the graph heterogeneity. Indeed, the ratio

$$\kappa = \frac{\langle k^2 \rangle}{\langle k \rangle} \tag{16}$$

is the parameter defining the level of heterogeneity of the network, since the normalized degree variance can be expressed as $\kappa/\langle k \rangle - 1$ and therefore high levels of fluctuations correspond to $\kappa \gg 1$. In homogeneous networks with a Poisson degree distribution, in which $\kappa = \langle k \rangle + 1$ we recover the result $\tau = (\lambda \langle k \rangle)^{-1}$, corresponding to the homogeneous mixing hypothesis. On the other hand, in networks with very heterogeneous connectivity patterns, κ is very large and the outbreak time-scale τ is very small, signaling a very fast diffusion of the infection. In particular, in scale-free networks characterized by a degree exponent $2 < \gamma \leq 3$ we have that $\kappa \sim \langle k^2 \rangle \rightarrow \infty$ with the network size $N \rightarrow \infty$. Therefore in uncorrelated scale-free networks we face a virtually instantaneous rise of the epidemic incidence. For large real-world networks, $\tau \rightarrow 0$ implies that the time-scale associated with the network is dominated by the finite size of the network ($\langle k^2 \rangle$ will be very large but finite) and is thus very small. In this case, the propagation time-scale is likely to have a lower cut-off generally set by other features of the spreading processes not related to the topology of the network.

3.3. Extension to the SIS and SIR models

It is worth stressing that the above results can be easily extended to the SIS and the SIR models (Anderson and May, 1992). In the case of uncorrelated networks, Eq. (9) contains, for both the SIS and the SIR models, an extra term $-\mu i_k(t)$ defining the rate at which infected individuals of degree k recover and become again susceptible or permanently immune and thus removed from the population, respectively:

$$\frac{di_k(t)}{dt} = \lambda k s_k(t) \Theta_k(t) - \mu i_k(t). \tag{17}$$

In the SIS model we have, as usual, $s_k(t) = 1 - i_k(t)$. In the SIR model, on the other hand, the normalization imposes that $s_k(t) = 1 - i_k(t) - r_k(t)$, where $r_k(t)$ is the density of removed individuals of degree k . The inclusion of the decaying term $-\mu i_k$, does not change the picture obtained in the SI model. By using the same approximations, the time-scale is found to behave as

$$\tau \sim \frac{\langle k \rangle}{\lambda \langle k^2 \rangle - (\mu + \lambda) \langle k \rangle}. \tag{18}$$

In the case of diverging fluctuations the time-scale behavior is therefore still dominated by $\langle k^2 \rangle$ and τ is always positive and going to 0 as $\langle k^2 \rangle \rightarrow \infty$ whatever

the spreading rate λ . This allows to recover the absence of an epidemic threshold, i.e. the lack of a decreasing prevalence region in the parameter space. It must be noted, however, that if fluctuations are not diverging, the outbreak time-scale is slightly different for the SIS and SIR models (Eq. (18)) than for the SI model (Eq. (15)).

3.4. Heterogeneous correlated networks

While we have so far restricted our study to the case of uncorrelated networks, it is worth noting that many real networks do not fill this assumption (Dorogovtsev and Mendes, 2003; Pastor-Satorras and Vespignani, 2004). In order to consider the presence of non-trivial correlations we have to fully take into account the structure of the conditional correlation function $P(k'|k)$. The equations we have written for the evolution of i_k in the SI model can therefore be stated as (Boguñá et al., 2003a,b)

$$\begin{aligned} \frac{di_k(t)}{dt} &= \lambda[1 - i_k(t)]k\Theta_k(t), \\ \Theta_k &= \sum_{k'} \frac{k' - 1}{k'} P(k'|k)(i_{k'}(t) - i_{k'}(0)) \\ &\quad + \sum_{k'} P(k'|k)i_{k'}(0). \end{aligned} \tag{19}$$

Here the Θ_k function takes into account explicitly the structure of the conditional probability that an infected vertex with degree k' points to a vertex of degree k , with any of the $k' - 1$ free edges it has (not pointing to the original source of its infection). In the absence of correlations, it is possible to see that $P(k'|k) = k'P(k')/\langle k \rangle$, recovering the results of Section 3.2. If the network presents correlations, measured by $P(k'|k)$, the situation is slightly more complex. The rate equation for $i_k(t)$ can be written in this case, neglecting terms of order $\mathcal{O}(i^2)$, as

$$\begin{aligned} \frac{di_k(t)}{dt} &= \sum_{k'} \lambda k \frac{k' - 1}{k'} P(k'|k)i_{k'}(t) + \lambda k \sum_{k'} \frac{i_{k'}(0)}{k'} P(k'|k) \\ &\equiv \sum_{k'} C_{k,k'} i_{k'}(t) + \lambda k \sum_{k'} P(k'|k) \frac{i_{k'}(0)}{k'}, \end{aligned} \tag{20}$$

which is a linear systems of differential equations governed by the matrix $\mathbf{C} = \{C_{k,k'}\}$ of elements

$$C_{k,k'} = \lambda k \frac{k' - 1}{k'} P(k'|k). \tag{21}$$

Elementary considerations from mathematical analysis tell us that the behavior of $i_k(t)$ will be given by a linear combination of exponential functions of the form $\exp(A_i t)$, where A_i are the eigenvalues of the matrix \mathbf{C} . Therefore, the dominant behavior of the averaged prevalence will be

$$i(t) \sim e^{A_m t}, \tag{22}$$

where A_m is the largest eigenvalue of the matrix \mathbf{C} . In the case of an uncorrelated network, we have that $C_{k,k'}^{nc} = \lambda k(k' - 1)P(k')/\langle k \rangle$, which has a unique eigenvalue satisfying

$$\sum_{k'} C_{k,k'} \Psi_{k'} = A_m^{nc} \Psi_k, \tag{23}$$

where $A_m^{nc} = \lambda(\langle k^2 \rangle / \langle k \rangle - 1)$, and where the corresponding eigenvector is $\Psi_k = k$, thus recovering the previous result Eq. (15) for this kind of networks.

In the case of correlated networks, it has been shown using the Frobenius theorem (Gantmacher, 1974) that the largest eigenvalue is bounded from below (Boguñá et al., 2003a,b)

$$A_m^2 \geq \min_k \sum_{k'} \sum_l (k' - 1)(l - 1)P(l|k)P(k'|l). \tag{24}$$

This equation is very interesting since it can be rewritten as

$$A_m^2 \geq \min_k \sum_l (l - 1)P(l|k)(k_{mm}(l) - 1). \tag{25}$$

It has been shown (Boguñá et al., 2003a,b) that, for scale-free network with $2 \leq \gamma \leq 3$, $k_{mm}(l)$ diverges for infinite size systems ($N \rightarrow \infty$). This ensures that also A_m diverges. Two particular cases have however to be treated separately: it may happen that, for some k_0 , $P(l|k_0) = 0$; then the previous limit for A_m^2 gives no information but it is then possible to show with slightly more involved calculations that A_m still diverges for $N \rightarrow \infty$ (Boguñá et al., 2003a,b). Another problem arises if $k_{mm}(l)$ diverges only for $l = 1$; this happens however only in particular networks where the singularity is accumulated in a pathological way onto vertices with a single edge. Explicit examples of this situation are provided in (Vázquez and Moreno, 2003).

The previous result has the important consequence that, even in the presence of correlations, the time-scale $\tau \sim 1/A_m$ tends to zero in the thermodynamic limit for any scale-free network with $2 < \gamma \leq 3$. It also underlines the relevance of the quantity k_{mm} , which gives a lower-bound for A_m in finite networks. In the next sections we will analyse numerically both the SI and SIS models in order to provide a full account of the dynamical properties that takes into account the network's complexity as well as finite size effects in the population.

4. Numerical simulations

In order to test the analytical predictions made in the previous sections, we have performed extensive numerical simulations of the SI and the SIS model in two different paradigmatic examples of complex network models with homogeneous and heterogeneous properties. The choice of the network models was dictated by

the request of generating an uncorrelated network, to fully exploit the analytical predictions. Simulations use an agent-based modeling strategy in which at each time step the SI dynamics is applied to each vertex by considering the actual state of the vertex and its neighbors. It is then possible to measure the evolution of the number of infected individuals and other quantities. In addition, given the stochastic nature of the model, different initial conditions and networks realizations can be used to obtain averaged quantities. In our simulations, we use $N = 10^4$ and $\langle k \rangle$ ranging from 4 to 20. We typically average our results for a few hundred networks while for each network, we average over a few hundreds different initial conditions.

4.1. Homogeneous networks

The example of homogeneous complex network we have chosen is the random graph model proposed by Erdős and Rényi (1959) (see e.g. Bollobás, 1985). The network is constructed from a set of N different vertices, in which each one of the $N(N - 1)/2$ possible edges is present with probability p (the connection probability), and absent with probability $1 - p$. This procedure results in a random network with average degree $\langle k \rangle = pN$ and a Poisson degree distribution in the limit of large N and constant $\langle k \rangle$,

$$P(k) = e^{-\langle k \rangle} \frac{\langle k \rangle^k}{k!}. \tag{26}$$

For $\langle k \rangle > 1$, it can be proved that the network exhibits a *giant component*, that is, a set of connected vertices whose size is proportional to N . In an actual realization, however, it is possible to generate networks in which a

fraction of the vertices belong to disconnected clusters. Therefore, we make the computer simulations of the spreading models only on the giant component.

In the case of the random graph, we checked the validity of Eq. (8), and that the time-scale is given by $1/\lambda\langle k \rangle$, as can be seen in Fig. (3).

Needless to say, in the case of a homogeneous network, the hypothesis $k \simeq \langle k \rangle$ captures the correct dynamical behavior of the spreading. This is a standard result and we report the numerical simulations just as a reference for comparison with the following numerical experiments on heterogeneous networks.

4.2. Heterogeneous networks

As a typical example of heterogeneous network, we have chosen the networks generated with the Barabási–Albert (BA) algorithm (Barabási and Albert, 1999). In this algorithm, the network starts from a small core of m_0 connected vertices. At each time step a new vertex is added, with m edges ($m < m_0$) connected to the old vertices in the network. The new edges are connected to an old vertex i with a probability proportional to its degree k_i (*preferential attachment*). The networks generated by this algorithm have a minimum degree m , an average degree $\langle k \rangle = 2m$, a scale-free degree distribution $P(k) \sim k^{-3}$ and vanishingly small correlations (Pastor-Satorras and Vespignani, 2004). In our simulations we use different network sizes N and minimum degree values m in order to change the level of heterogeneity, that in this case is given by $\kappa \sim m \ln N$.

In the simulation we keep track of the average density of infected individuals versus time for a network generated with the preferential attachment rule. In Fig. 4 we show a typical result and the fitting procedure which allows us to measure the value of τ .

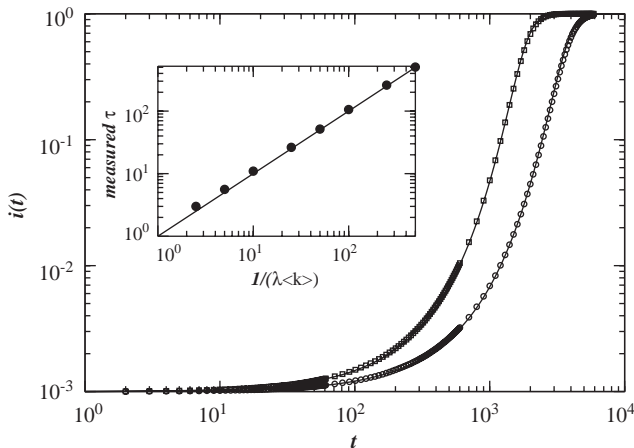


Fig. 3. Main frame: the symbols correspond to simulations of the SI model with $\lambda = 10^{-4}$ on ER networks with $N = 10^4$, $\langle k \rangle = 20, 40$; the lines are fits of the form of Eq. (8). Inset: measured time-scale τ , as obtained from fitting, versus the theoretical prediction for different values of $\langle k \rangle$ and λ .

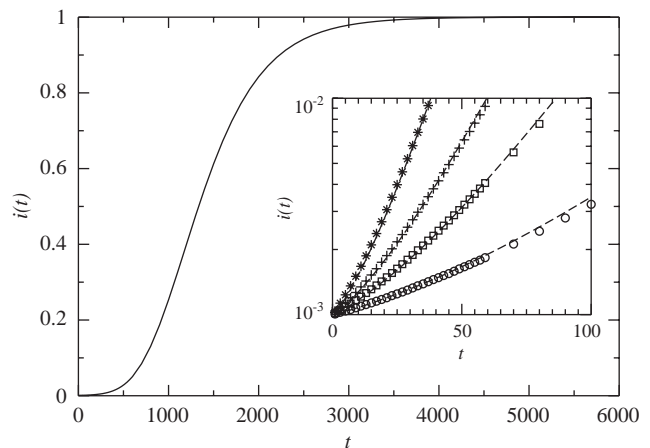


Fig. 4. Average density of infected individuals versus time in a BA network of $N = 10^4$ with $m = 2$. The inset shows the exponential fit obtained in the early times (lines) and the numerical curves $i(t)$ for networks with $m = 4, 8, 12, 20$ (from bottom to top).

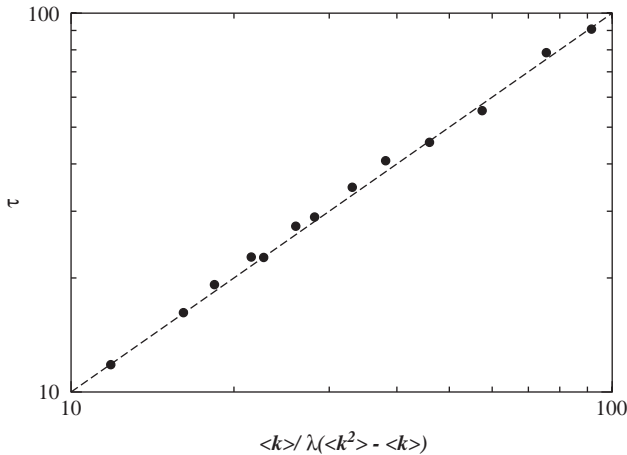


Fig. 5. Measured time-scale τ in BA networks as obtained from exponential fitting versus the theoretical prediction for different values of m and N corresponding to different levels of heterogeneity.

In Fig. 5 we report the early time behavior of outbreaks in networks with different heterogeneity levels and the behavior of the measured τ with respect to $\langle k \rangle / \lambda(\langle k^2 \rangle - \langle k \rangle)$. The numerical results recover the analytical prediction with great accuracy. Indeed, the BA network is a good example of uncorrelated heterogeneous network in which the approximations used in the calculations are satisfied. In networks with correlations we expect to find different quantitative results but a qualitatively similar framework as it happens in the case of the epidemic threshold evaluation (Boguñá et al., 2003a,b).

4.3. The SIS dynamics

As claimed in previous sections, we have tested that at short times and for large heterogeneous networks ($\kappa \gg 1$), the SI model is a good approximation to the more general SIS model described by Eq. (17). In Fig. 6 we plot $i(t)$ versus t for a simulation of the SI and the SIS model with $\lambda = 10^{-3}$, on a BA network with $m = 8$ and $N = 10^4$, corresponding to $\langle k \rangle = 16$ and $\langle k^2 \rangle \approx 632$. We took different values for the parameter μ : $\mu = 0$ (which corresponds to the SI model), $\mu = 10^{-4}$, 10^{-3} , 10^{-2} ; Eq. (18) yields the following values for τ : $\tau(\mu = 0) \approx 26$, $\tau(\mu = 0.0001) \approx 26.1$, $\tau(\mu = 0.001) \approx 26.7$, $\tau(\mu = 0.01) \approx 35$. Fig. 6 clearly shows that indeed for $\mu(k) \ll \lambda(k^2)$ and short times the curves are indistinguishable so that the SIS model is well described by the SI approximation in this regime. As μ gets larger the behavior changes since the time-scale of the recovery is no longer much larger than the other time-scales. It is possible to show that the same results apply also in the case of the SIR model.

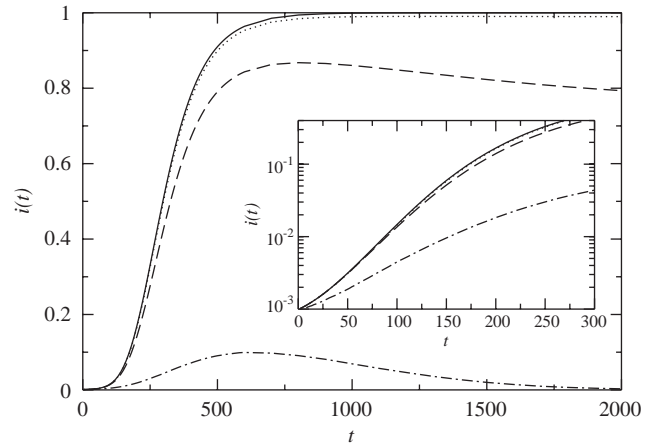


Fig. 6. SIS model on a BA network with $N = 10^4$, $m = 8$; $\lambda = 10^{-3}$, and $\mu = 0, 10^{-4}, 10^{-3}, 10^{-2}$ from top to bottom. The inset focuses on the short-time dynamics: the curve is superimposed on data for the SI model up to more than 10τ ($\mu = 0$) for $\mu = 10^{-4}$ and up to a few times $\tau(\mu = 0)$ for $\mu = 10^{-3}$.

5. The infection time pattern: the cascade effect

The previous results show that the heterogeneity of scale-free connectivity patterns favors epidemic spreading not only by suppressing the epidemic threshold, but also by accelerating the epidemic propagation in the population. The velocity of the spreading leaves us with very short response times in the deployment of control measures and a detailed knowledge of the way epidemics propagate through the network could be very valuable in the definition of adaptive strategies. Indeed, the epidemic diffusion is far from homogeneous. The simple formal integration of Eq. (9) written for $s_k = 1 - i_k$ yields

$$s_k(t) = s_k^0 e^{-\lambda k \Phi(t)}, \tag{27}$$

where $\Phi(t) = \int_0^t dt' \Theta(t')$. This result is valid for any value of the degree k and the function $\Phi(t)$ is positive and monotonously increasing. This last fact implies that s_k is decreasing monotonously towards zero when time grows. Thus, if one has two values $k > k'$ and whatever the initial conditions s_k^0 and $s_{k'}^0$, there is a time t_x after which $s_k(t) < s_{k'}(t)$. This ‘crossing’ time is given by

$$\phi(t_x) = \frac{1}{\lambda(k - k')} \log \left[\frac{s_k^0}{s_{k'}^0} \right]. \tag{28}$$

(If $s_k^0 < s_{k'}^0$, there is no crossing and for all times $s_k(t) < s_{k'}(t)$.) This result indicates that after an initial regime which depends on the initial conditions, the disease spreads always from large connectivity to smaller connectivities.

We can go beyond the analytical result that is necessarily grounded on average quantities by relying on numerical simulations. Indeed, a more precise

characterization of the epidemic diffusion through the network can be achieved by studying some convenient quantities that highlight the invasion pattern of the infection in numerical spreading experiments in BA networks. First, we measure the average degree of the newly infected nodes at time t , defined as

$$\bar{k}_{inf}(t) = \frac{\sum_k k[I_k(t) - I_k(t-1)]}{I(t) - I(t-1)}. \tag{29}$$

In Fig. 7 we plot this quantity for BA networks as a function of the rescaled time t/τ . The curves show an initial plateau that can be easily understood by considering that at very low density of infected individuals, each vertex will infect a fraction of its neighbors without correlations with the spreading from other vertices. In this case each edge points to a vertex with degree k with probability $kP(k)/\langle k \rangle$ and the average degree of newly infected vertices is given by

$$\bar{k}_{inf}(t) = \langle k^2 \rangle / \langle k \rangle. \tag{30}$$

After this initial regime, $\bar{k}_{inf}(t)$ decreases smoothly when time increases. The dynamical spreading process is therefore clear: after the hubs are very quickly infected the spread is going always towards smaller values of k . This is confirmed by the large time regime that settles in a plateau

$$\bar{k}_{inf}(t) = m, \tag{31}$$

which means that the vertices with the lowest degree are typically the last to be infected.

Further information on the infection propagation is provided by the inverse participation ratio $Y_2(t)$ (Derrida and Flyvbjerg, 1987; Barthélemy et al., 2002). We first define the weight of infected individuals in each degree class k by $w_k(t) = I_k(t)/I(t)$. The quantity Y_2 is

then defined as

$$Y_2(t) = \sum_k w_k^2(t). \tag{32}$$

If $Y_2 \sim 1/k_{max}$ (k_{max} is the maximal connectivity), infected vertices are homogeneously distributed among all degree classes. In contrast, if Y_2 is not small (of order $1/n$ with n of order unity) then the infection is localized on some specific degree classes that dominate the sum of Eq. (32). In Fig. 8 we report the behavior of Y_2 versus time for BA networks with different minimum degree. The function Y_2 has a maximum at the early time stage, indicating that the infection is localized on the large k classes, as we infer from the plot of $\bar{k}_{inf}(t)$, see Fig. 7. First Y_2 decreases, with the infection progressively invading lower degree classes, and providing a more homogeneous diffusion of infected vertices in the various k classes. Finally, the last stage of the process corresponds to the capillary invasion of the lowest degree classes which have a larger number of vertices and thus provide a larger weight. In the very large time limit, when the whole network is infected, $Y_2(t = \infty) = \sum_k P(k)^2$. Noticeably, curves for different levels of heterogeneity have the same time profile in the rescaled variable t/τ . This implies that, despite the various approximations used in the calculations, the whole spreading process is dominated by the time-scale defined in the early exponential regime of the outbreak.

The presented results provide a clear picture of the infection propagation in heterogeneous networks. First the infection takes control of the large degree vertices in the network. Then it rapidly invades the network via a cascade through progressively smaller degree classes. The dynamical structure of the spreading is therefore characterized by a hierarchical cascade from hubs to intermediate k and finally to small k classes.

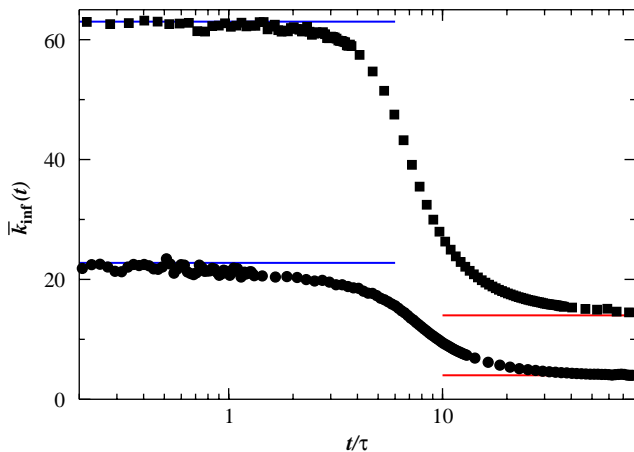


Fig. 7. Time behavior of the average degree of the newly infected nodes for SI outbreaks in BA networks (here of size $N = 10^4$). Time is rescaled by τ . Reference lines are drawn at the asymptotic values $\langle k^2 \rangle / \langle k \rangle$ for $t \leq \tau$ and m for $t \geq \tau$. The two curves are for $m = 4$ (bottom) and $m = 14$ (top).

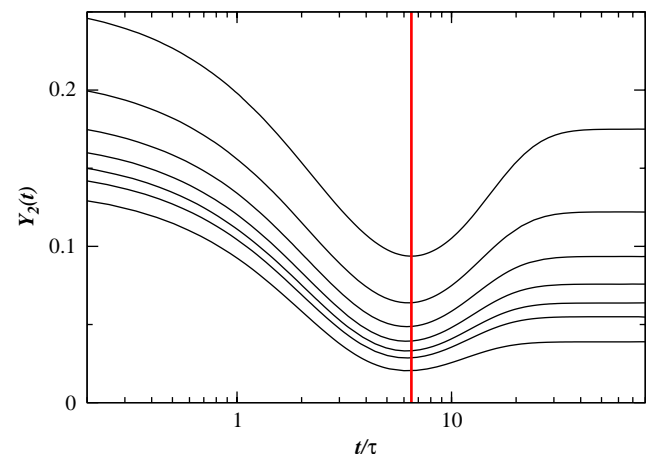


Fig. 8. Inverse participation ratio Y_2 versus time for BA network of size $N = 10^4$ with minimum degree $m = 4, 6, 8, 10, 12, 14$ and 20 , from top to bottom. Time is rescaled with τ . The reference line indicates the minimum of Y_2 around $t/\tau \simeq 6.5$.

6. The effect of the initial seed of the infection

In very heterogeneous networks it is reasonable to forecast that epidemic outbreaks starting from individuals possessing very different connectivity properties may undergo a rather different time evolution. In order to investigate in more detail the effect of initial conditions, one can write the general solution of Eqs. (12) with $i_k(t = 0) = f(k)$ where f is some given function of the degree

$$i_k(t) = f(k) + k\Theta_0 \frac{\langle k \rangle}{\langle k^2 \rangle - \langle k \rangle} [e^{t/\tau} - 1], \quad (33)$$

where $\Theta_0 = \Theta(t = 0) = \langle kf(k) \rangle / \langle k \rangle$. Comparing this last expression with Eq. (13), we conclude that, apart from the effect of the initial density of infected individuals, the only effect in the dynamics is the presence of the prefactor Θ_0 , which implies that the spreading is faster for larger Θ_0 . In the particular case in which the initial infection is located on N_0 vertices of given degree k_0 , we obtain $i_{k_0}(t = 0) = N_0 / (NP(k_0))$ and thus $\Theta_0 = k_0 N_0 / (N \langle k \rangle)$. Analogously it is easy to see that, for N_0 initially contaminated sites, all with connectivity larger than a certain k_M , Θ_0 is proportional both to N_0 / N and to k_M .

Eq. (33) clearly highlights the role of the large connectivity sites: on the one hand, for a given initial condition, the infection of classes with larger k leads to faster rise of the epidemic; on the other hand, the larger the degree of the initially infected sites, the faster the propagation of the epidemics. Note however that the time-scale τ itself is not affected by the initial conditions, which appear through the prefactors only. Using Eq. (33) we can highlight these features since the right-hand side of the expression

$$\frac{i_k(t) - f(k)}{k\Theta_0} = \frac{\langle k \rangle}{\langle k^2 \rangle - \langle k \rangle} [e^{t/\tau} - 1] \quad (34)$$

has to be independent on both the initial conditions (which enter i_k only through $f(k)$ and Θ_0) and the degree k . We have verified this in Fig. 9, by means of numerical simulations of the SI model on BA networks with specific initial conditions: if the spreading starts from N_0 infected sites of connectivity k_0 , Θ_0 is proportional to N_0 and k_0 , so that we show that the quantity

$$\frac{i_k(t) - f(k)}{kN_0k_0} \quad (35)$$

is independent of k and k_0 , and is also equal to

$$\frac{i(t) - i_0}{\langle k \rangle N_0 k_0}. \quad (36)$$

At large times the curves separate since the expression (13) is no longer valid. The data collapse of Fig. 9 once again shows the validity of the analytical approach developed in Section 3. The time-scale τ for the

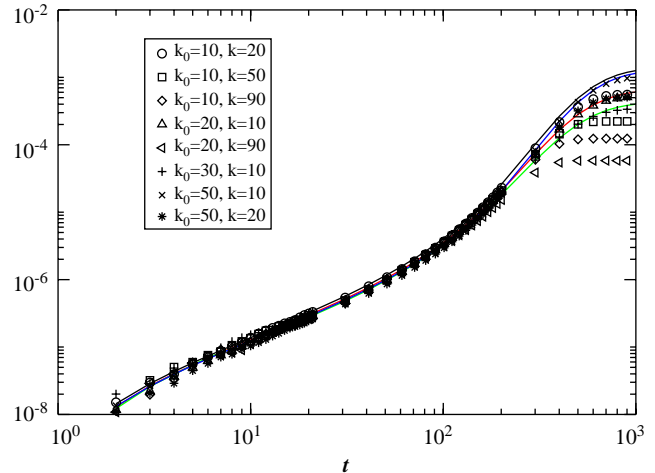


Fig. 9. Collapse plot of quantities (35) and (36) versus time for the SI model on a BA network, with initial conditions given by N_0 infected sites having a given connectivity k_0 . Here $N_0 = 10$, $N = 10^4$. The data are averaged over 200 realizations of the network and 50 runs on each network sample. Lines correspond to (36) for $k_0 = 10, 20, 30, 50$; symbols correspond to (35) for the same initial conditions and various values of k between 10 and 90 (The maximal connectivity is of order $\sqrt{N} = 100$).

exponentially fast outbreak of the epidemics is relevant for any kind of initial conditions and for all nodes, independently from their connectivity. The prefactors however show that the spreading is faster if the infected seeds have a large connectivity and, among the connectivity classes, hubs are typically infected faster.

7. Fluctuations: the relevance of τ for single case studies

The previous results are valid for the average density of infected nodes and it is legitimate to ask about the relevance of these results to the case of a single network sample. Indeed, in the real-world there is not such a thing as averages over different network realizations and we have to check the robustness of our results on a single network sample. It is then natural to wonder if large statistical fluctuations in the network structure may reverberate on the difference between single case studies and asymptotic average results. In particular, we can compare the previously defined time-scale τ (Eq. (15)), which corresponds to the exponential growth of the prevalence averaged over the networks statistical properties and initial conditions, with an operative measure of time-scale obtained in a single network realization case study. For a given network, and starting from a given initial density of infected vertices i_0 , we define for each run of the spreading process the typical realization time-scale as the time τ' at which the density of infected nodes $i_{run}(t)$ in the specific run is equal to the average quantity $i(t)$ at time τ provided by Eq. (14). This

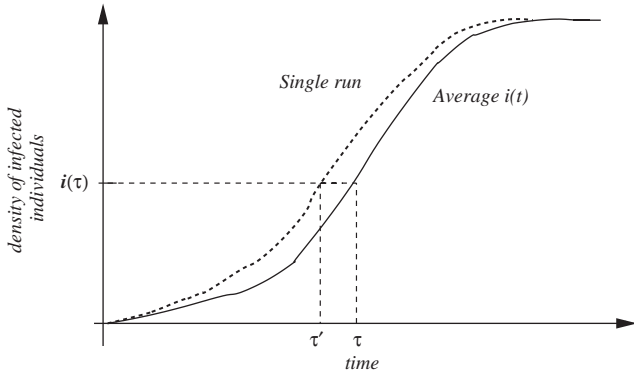
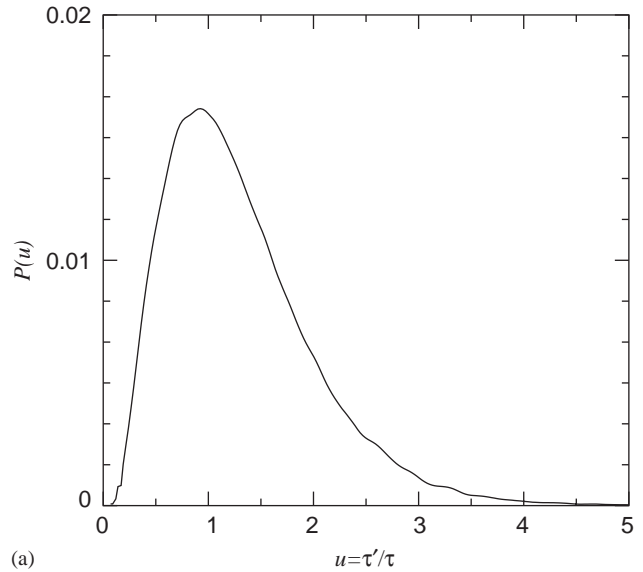


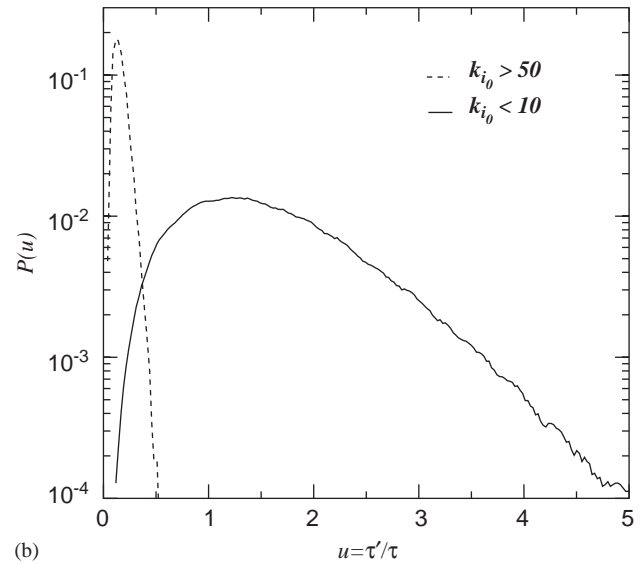
Fig. 10. Schematic definition of τ' for a single run. Given the average density $i(t)$, τ' is defined as the time in which the density of a given run reaches $i(\tau)$.

defines τ' as the effective time at which $i_{run}(t = \tau') = i(t = \tau)$ (see Fig. 10). The deviation from the average behavior in each run can be readily accounted by the variable $u = \tau'/\tau$ which is a simple measure of the relevance of τ for each run. In Fig. 11(a), we plot the probability distribution of u computed for a given realization of the network. This figure shows that $P(u)$ is not broadly distributed. In other words it is very unlikely to find large deviations of u from the unity, at which the distribution is strongly peaked. This evidence indicates that even if fluctuations are possible, the time-scale defined by τ is a meaningful characterization of the spreading process.

A more detailed analysis highlights once more the key role of initial conditions in the epidemics spread. In Fig. 11(b), we used the same network as in Fig. 11(a), but we made the following distinction according to the connectivity of the initially infected nodes. We used initial conditions (i) with small connectivity $k < 10$ and (ii) with large connectivity $k > 50$ (the maximal connectivity of the network is 100 in this case). Fig. 11(b) shows that the condition (ii) is the main contribution to the small $u < 1$ values while it is the condition (i) which contributes mostly to the larger values $u > 1$. These results can be easily explained as follows: We know from previous sections that the first steps of the epidemics process are concerning the hubs' infection. In the case (i), the path from the infected seeds to the hubs can be long and can thus induce a slower growth in $i(t)$. In the opposite case (ii), instead, the seeds are mainly located on the hubs since the beginning and the initial outbreak is generally faster than the average. This clear difference tells us that statistical deviations from the average time-scale τ can be traced back to the initial conditions of the epidemics. In this perspective, the specific network realizations appear to have a rather small influence on statistical fluctuations. This last feature is due to the intrinsic large amount of connectivity fluctuations that each network realization possesses in the case of a very heterogeneous topology. Additional fluctuations, such as those stem-



(a)



(b)

Fig. 11. Probability distribution of $u = \tau'/\tau$. (a) For a given network with random initial conditions (the BA network is obtained for $N = 10^4$, $m = 2$, and 1000 realizations). (b) Probability distribution of u for different initial conditions: in full lines the nodes initially infected have a connectivity $k < 10$ and in dashed lines $k > 50$ (here $k_{max} = 100$).

ming from the specific realization and finite size, are thus a higher order correction to the intrinsic statistical fluctuations which are accounted for correctly in the theoretical description.

More generally, these results show that initial conditions induce fluctuations in the outbreak time which are never 'large' in the sense that $P(u)$ decays rapidly, which implies that the time-scale τ is relevant even for a single realization of the network. This result is important since in real world situations, the disease spreads on one single network and it has to be checked whether results obtained on average are relevant or not.

8. Conclusions

In this paper, we have provided a general picture of the effect of complex connectivity patterns in the spreading dynamics of epidemic phenomena. We have shown how the large connectivity fluctuations present in a large class of population networks lead to a novel epidemiological framework in which both the epidemic threshold and the growth time-scale of the outbreak do not have an intrinsic value. Indeed, the virtual lack of epidemic threshold and instantaneous rising of the prevalence in infinitely large networks corresponds to non-intrinsic quantities depending on the specific system size of the actual population. In addition, the dynamical structure of the spreading process is characterized by a hierarchical cascade from hubs to intermediate k and finally to small k vertices. That is, the infection first takes place on the subset of individuals with the largest number of contacts, and then progressively invades individuals with decreasing number of contacts. The emerging picture might be of practical importance in the implementation and assessment of dynamic control strategies. In particular, an efficient way to stop epidemics could rely on a dynamical deployment of containment measures that focuses on progressively changing classes of the population. More specifically, our results confirm the importance of control strategies targeting the hubs of the population but also highlight the fact that global surveillance is a major key aspect of epidemics control and that immunization strategies have to evolve with time during the different phases of the spread.

Acknowledgements

A.B., A.V. and R.P.-S. are partially funded by the European Commission—Fet Open project COSIN IST-2001-33555. R.P.-S. acknowledges financial support from the Ministerio de Ciencia y Tecnología (Spain), and from the Departament d'Universitats, Recerca i Societat de la Informació, Generalitat de Catalunya (Spain).

References

- Albert, R., Barabási, A.-L., 2002. Statistical mechanics of complex networks. *Rev. Mod. Phys.* 74, 47–97.
- Amaral, L.A.N., Scala, A., Barthélemy, M., Stanley, H.E., 2000. Classes of small-world networks. *Proc. Natl Acad. Sci. USA* 97, 11149–11152.
- Anderson, R.M., May, R.M., 1992. *Infectious Diseases in Humans*. Oxford University Press, Oxford.
- Bailey, N.T.J., 1975. *The Mathematical Theory of Infectious Diseases*, second ed. Griffin, London.
- Barabási, A.-L., Albert, R., 1999. Emergence of scaling in random networks. *Science* 286, 509–511.
- Barrat, A., Barthélemy, M., Pastor-Satorras, R., Vespignani, A., 2004. The architecture of complex weighted networks. *Proc. Natl Acad. Sci. USA* 101, 3747–3752.
- Barthélemy, M., Gondran, B., Guichard, E., 2002. Spatial structure of the internet traffic. *Physica A* 319, 633–642.
- Barthélemy, M., Barrat, A., Pastor-Satorras, R., Vespignani, A., 2004. Velocity and hierarchical spread of epidemic outbreaks in scale-free networks. *Phys. Rev. Lett.* 92, 178701.
- Boguñá, M., Pastor-Satorras, R., 2002. Epidemic spreading in correlated complex networks. *Phys. Rev. E* 66, 047104.
- Boguñá, M., Pastor-Satorras, R., Vespignani, A., 2003a. Absence of epidemic threshold in scale-free networks with degree correlations. *Phys. Rev. Lett.* 90, 028701.
- Boguñá, M., Pastor-Satorras, R., Vespignani, A., 2003b. Epidemic spreading in complex networks with degree correlations. In: Pastor-Satorras, R., Rubí, J.M., Díaz-Guilera, A. (Eds.), *Statistical Mechanics of Complex Networks*. Lecture Notes in Physics, vol. 625. Springer, Berlin.
- Bollobás, B., 1985. *Random Graphs*. Academic Press, London.
- Cohen, R., Havlin, S., 2003. Scale-free networks are ultrasmall. *Phys. Rev. Lett.* 90, 058701.
- Colgate, S.A., Stanley, E.A., Hyman, J.M., Layne, S.P., Qualls, C., 1989. Risk behavior-based model of the cubic growth of acquired immunodeficiency syndrome in the United States. *Proc. Natl Acad. Sci. USA* 86, 4793–4797.
- Dailey, D.J., Gani, J., 2001. *Epidemic Modelling: An Introduction*. Cambridge University Press, Cambridge.
- Derrida, B., Flyvbjerg, H., 1987. Statistical properties of randomly broken objects and of multivalley structures in disordered systems. *J. Phys. A: Math. Gen.* 20, 5273–5288.
- Dezsö, Z., Barabási, A.-L., 2002. Halting viruses in scale-free networks. *Phys. Rev. E* 65, 055103(R).
- Diekmann, O., Heesterbeek, J.A.P., 2000. *Mathematical Epidemiology of Infectious Diseases: Model Building, Analysis and Interpretation*. Wiley, New York.
- Dorogovtsev, S.N., Mendes, J.F.F., 2003. *Evolution of Networks: From Biological Nets to the Internet and WWW*. Oxford University Press, Oxford.
- Erdős, P., Rényi, P., 1959. On random graphs. *Publ. Math.* 6, 290–297.
- Eubank, S., Guclu, H., Kumar, A., Marathe, M.V., Srinivasan, A., Toroczkai, Z., Wang, N., 2004. Modelling disease outbreaks in realistic urban social networks. *Nature* 429, 180–184.
- Ferguson, N.M., Keeling, M.J., Edmunds, W.J., Gani, R., Greenfell, B.T., Anderson, R.M., 2003. Planning for smallpox outbreaks. *Nature* 425, 681–685.
- Gantmacher, F.R., 1974. *The Theory of Matrices*, vol. II. Chelsea Publishing Company, New York.
- Guimerà, R., Mossa, S., Turtchi, A., Amaral, L.A.N., 2003. Structure and efficiency of the world-wide airport network. e-print cond-mat/0312535.
- Hethcote, H.W., Yorke, J.A., 1984. Gonorrhoea: transmission and control. *Lect. Notes Biomath.* 56, 1–105.
- Liljeros, F., Edling, C.R., Amaral, L.A.N., Stanley, H.E., Aberg, Y., 2001. The web of human sexual contacts. *Nature* 411, 907–908.
- Lloyd, A.L., May, R.M., 2001. How viruses spread among computers and people. *Science* 292, 1316–1317.
- May, R.M., Anderson, R.M., 1984. Spatial heterogeneity and the design of immunization programs. *Math. Biosci.* 72, 83–111.
- May, R.M., Anderson, R.M., 1988. The transmission dynamics of human immunodeficiency virus (HIV). *Philos. Trans. Roy. Soc. London B* 321, 565.
- May, R.M., Lloyd, A.L., 2001. Infection dynamics on scale-free networks. *Phys. Rev. E* 64, 066112.
- Moreno, Y., Pastor-Satorras, R., Vespignani, A., 2002. Epidemic outbreaks in complex heterogeneous networks. *Eur. Phys. J. B* 26, 521–529.

- Murray, J.D., 1993. *Mathematical Biology*, second ed. Springer, Berlin.
- Newman, M.E.J., 2002a. Spread of epidemic disease on networks. *Phys. Rev. E* 66, 016128.
- Newman, M.E.J., 2002b. Assortative mixing in networks. *Phys. Rev. Lett.* 89, 208701.
- Pastor-Satorras, R., Vespignani, A., 2001a. Epidemic spreading in scale-free networks. *Phys. Rev. Lett.* 86, 3200–3203.
- Pastor-Satorras, R., Vespignani, A., 2001b. Epidemic dynamics and endemic states in complex networks. *Phys. Rev. E* 63, 066117.
- Pastor-Satorras, R., Vespignani, A., 2004. *Evolution and Structure of the Internet: A Statistical Physics Approach*. Cambridge University Press, Cambridge.
- Schneeberger, A., Mercer, C.H., Gregson, S.A.J., Ferguson, N.M., Nyamukapa, C.A., Anderson, R.M., Johnson, A.M., Garnett, G.P., 2004. Scale-free networks and sexually transmitted diseases. *Sex. Transm. Dis.* 31, 380–387.
- Vázquez, A., Moreno, Y., 2003. Disease spreading in structured scale-free networks. *Eur. Phys. J. B* 31, 265–271.
- Yorke, J.A., Hethcote, H.W., Nold, A., 1978. Dynamics and control of the transmission of gonorrhoea. *Sex. Transm. Dis.* 5, 51–56.